

# **SANDIA REPORT**

SAND98-0564 • UC-712

Unlimited Release

Printed March 1998

## **Development of a Cryogenic EOS Capability for the Z Pulsed Radiation Source:**

## **Goals and Accomplishments of FY97 LDRD Project**

David L. Hanson, Robert R. Johnston, James R. Asay

Prepared by

Sandia National Laboratories

Albuquerque, New Mexico 87185 and Livermore, California 94550

Sandia is a multiprogram laboratory operated by Sandia Corporation,  
a Lockheed Martin Company, for the United States Department of  
Energy under Contract DE-AC04-94AL85000.

Approved for public release; further dissemination unlimited.



**Sandia National Laboratories**

Issued by Sandia National Laboratories, operated for the United States Department of Energy by Sandia Corporation.

**NOTICE:** This report was prepared as an account of work sponsored by an agency of the United States Government. Neither the United States Government nor any agency thereof, nor any of their employees, nor any of their contractors, subcontractors, or their employees, makes any warranty, express or implied, or assumes any legal liability or responsibility for the accuracy, completeness, or usefulness of any information, apparatus, product, or process disclosed, or represents that its use would not infringe privately owned rights. Reference herein to any specific commercial product, process, or service by trade name, trademark, manufacturer, or otherwise, does not necessarily constitute or imply its endorsement, recommendation, or favoring by the United States Government, any agency thereof, or any of their contractors or subcontractors. The views and opinions expressed herein do not necessarily state or reflect those of the United States Government, any agency thereof, or any of their contractors.

Printed in the United States of America. This report has been reproduced directly from the best available copy.

Available to DOE and DOE contractors from  
Office of Scientific and Technical Information  
P.O. Box 62  
Oak Ridge, TN 37831

Prices available from (615) 576-8401, FTS 626-8401

Available to the public from  
National Technical Information Service  
U.S. Department of Commerce  
5285 Port Royal Rd  
Springfield, VA 22161

NTIS price codes  
Printed copy: A04  
Microfiche copy: A01

# **Development of a Cryogenic EOS Capability for the Z Pulsed Radiation Source:**

## **Goals and Accomplishments of FY97 LDRD Project**

**David L. Hanson and Robert R. Johnston**  
**Ion Beam Physics Department**

**James R. Asay**  
**Shock Physics Applications Department**

**Sandia National Laboratories**  
**P.O. Box 5800**  
**Albuquerque, NM 87185-1186**

### **Abstract**

Experimental cryogenic capabilities are essential for the study of ICF high-gain target and weapons effects issues involving dynamic materials response at low temperatures. This report describes progress during the period 2/97-11/97 on the FY97 LDRD project "Cryogenic EOS Capabilities on Pulsed Radiation Sources (Z Pinch)". The goal of this project is the development of a general purpose cryogenic target system for precision EOS and shock physics measurements at liquid helium temperatures on the Z accelerator Z-pinch pulsed radiation source. Activity during the FY97 LDRD phase of this project has focused on development of a conceptual design for the cryogenic target system based on consideration of physics, operational, and safety issues, design and fabrication of principal system components, construction and instrumentation of a cryogenic test facility for off-line thermal and optical testing at liquid helium temperatures, initial thermal testing of a cryogenic target assembly, and the design of a cryogenic system interface to the Z pulsed radiation source facility. We discuss these accomplishments as well as elements of the project that require further work.



## Acknowledgments

We thank G. Yonas and the 9000 Discretionary LDRD Committee for funding part of this work; J. Seamen and D. Petmecky for assistance with Z operational issues; C. A. Hall and C. H. Konrad for useful discussions of EOS diagnostic requirements; M. K. Matzen, J. L. Porter, and B. N. Turman for programmatic support; and M. E. Cuneo for carefully reviewing this report.

# Contents

I.	Introduction	1
II.	Motivation for Cryogenic EOS Measurements	1
III.	Milestones and Accomplishments for FY97 Phase of Project	3
IV.	Conceptual Design for Cryogenic Target System	4
V.	Safety Issues	6
VI.	Cryogenic Test Facility	7
VII.	Cryostat Design	7
VIII.	Cryogenic Sample Holder Design	12
IX.	Cryogenic Target System Test Results	14
X.	Summary and Future Work	22
	References	24

# Figures

1.	Continuous flow LHe cryostat with LN <sub>2</sub> -cooled outer radiation shield. The sample holder is in direct thermal contact with the cryostat cold finger. ....	9
2.	Continuous flow LHe cryostat with LN <sub>2</sub> -cooled outer radiation shield. The sample holder is connected to the cryostat cold finger through a thermal link consisting of OFHC copper wire. ....	11
3.	Cryogenic sample holder (OFHC copper) for containing liquid samples (LH <sub>2</sub> , LD <sub>2</sub> ) condensed from the gas phase. A thermal break is provided between the sample holder and hohlraum. ....	12
4.	Cryogenic sample holder (OFHC copper) for cooling solid samples in the range of 6-30 K. ....	13
5.	Cryogenic sample holder (OFHC copper) with integrated cryostat for cooling samples to T < 6 K (additional radiation shielding not shown). ....	14

6. Cooling history of LN<sub>2</sub>-cooled cryostat outer shield (see Fig. 2). Shield temperature decreases from 82 K to 76.4 K as the LN<sub>2</sub> flow rate is reduced from 40 L/hr to 10 L/hr. .... 15
  
7. Cooling history of the LHe cryostat cold finger (see Fig. 2) during a temperature control test. The minimum cold finger temperature (5.3 K) is reached after sample holder cooldown to an equilibrium temperature of 20.1 K. The hold-time of the continuous flow LHe reservoir after LHe flow is cut off is about 5 min. .... 15
  
8. Cooling history of the LHe-cooled cryostat inner shield (see Fig. 2). Minimum temperature (4.4 K) is reached after sample holder cooldown. .... 17
  
9. Cooling history of a cryogenic sample holder (Fig. 4) during a temperature control test. The sample holder is connected to the cryostat cold finger through a 15-cm-long, 0.41-cm-diameter section of OFHC copper wire to provide standoff for blast protection of the cryostat (Fig. 2). The sample holder reaches an equilibrium temperature of 20.1 K in this configuration. .... 17
  
10. Demonstration of temperature control of the sample holder with standoff (expanded view of Fig. 9). The temperature controller setpoint is increased in 0.5 K steps and then in 2.5 K steps to 25 K and the sample holder temperature is maintained within 0.1 K of the setpoint for several minutes on each step. .... 18
  
11. Cooling history of the primary hohlraum connected to the sample holder through the thermal break and secondary hohlraum stub (see Figs. 4 and 9). .... 19
  
12. Pressure history in the cryogenic test facility vacuum chamber. The improvement in vacuum is a result of cryopumping by cryogenic target system components during the cooling test (Figs. 6-11). .... 19
  
13. Cooling history of the LHe cryostat cold finger (see Fig. 2) during another temperature control test. The minimum cold finger temperature (4.9 K) is reached after sample holder cooldown to an equilibrium temperature of 24.5 K. LHe consumption during the

	entire 210 minute LHe cooling sequence from cooldown to exhaustion of the LHe supply was 80 liters. ....	21
14.	Demonstration of temperature control of the sample holder with standoff. The sample holder is connected to the cryostat cold finger through a 20-cm-long, 0.41-cm-diameter section of OFHC copper wire. The temperature controller setpoint is increased in 10.0 K steps to 74.5 K and the sample holder temperature is maintained within 0.1 K of the setpoint for several minutes on each step. ....	21



# **I. Introduction**

The prediction and analysis of ICF high gain targets and other weapons physics issues require models of dynamic materials response that can accurately describe thermodynamic properties and high-rate mechanical phenomena over an extensive range of pressures and temperatures. For ICF materials, modeling capabilities validated by experimental data are needed at cryogenic temperatures, since most ICF designs are based on performance of cryogenic multi-shell capsules. The LDRD project “Cryogenic EOS Capabilities on Pulsed Radiation Sources (Z-pinch)” [1] was initiated in FY97 to develop a general purpose cryogenic target system for precision EOS and shock physics studies at liquid helium (LHe) temperatures on the Z Pulsed Radiation Source (PRS). A cryogenic target assembly for Z has to meet a number of requirements: (1) it must be capable of containing liquid samples, including hydrogen and deuterium, and also solid materials, such as polycarbonate and metallic ablaters for ICF; (2) it must include the capability to use various shock diagnostics, such as VISAR interferometry and shock velocity measurements; and (3) it must meet the operational and safety requirements for use on Z and, if possible, allow for the survival of high value cryogenic components in the Z debris environment. In FY97, we have concentrated on the design, fabrication, and bench testing of a fully functional cryogenic target system and integration of that target system into Z-pinch hohlraum experiments on Z. We plan to use the system developed as a result of this work for EOS measurements on solid targets (and possibly liquid deuterium) in FY98.

## **II. Motivation for Cryogenic EOS Measurements**

With the loss of underground testing and the recent developments in teraflop computing capability, there is increased emphasis to ensure that the nuclear weapons laboratories sustain the capability for predicting and analyzing the performance of nuclear weapons through computational-based approaches. Similar modeling requirements exist for the ICF program, since present high-gain fusion targets rely on critical timing of external radiation deposition to simultaneously optimize fuel compression in the ICF capsule and suppress formation of Rayleigh-Taylor instabilities during compression. Recent rad-hydro simulations of high-gain ICF targets at LLNL and SNL indicate that capsule yields can be significantly reduced by variations of a few percent in the sound speeds of capsule materials at high pressures. This information is not generally available, which forces reliance on models existing in the codes,

such as the Mie-Grueneisen model, which is known to contain inaccuracies for predicting off-Hugoniot properties, such as sound speeds.

The need to accurately model ICF capsule performance results in stringent requirements on condensed matter and dense plasma theories to adequately model materials over a broad dynamic range. The models must predict dynamic material response for pressures of several Mbar, temperatures of several eV, and for loading rates approaching the vibration times of atomic motions. The rapid loading rates produce deformation mechanisms and dissipative effects and phase transition kinetics that are not currently modeled well, but can significantly influence material motions (for example, refreezing from melted states may not occur in the implosion times of materials used in weapon primaries). For simple materials such as metals, these mechanisms involve dissipative processes such as the generation of dislocations and other defects that are important to kinetic processes such as dynamic yielding, melting, refreezing, polymorphic transitions, and tensile failure; all of these properties must be accurately predicted in applications involving the performance, safety, and reliability of nuclear weapons and some ICF geometries. In more complex materials, such as DT fuels and polycarbonates, it is also necessary to model and predict the effects of molecular dissociation. The present theoretical ability to model these effects is extremely limited. Consequently, computational based approaches for analysis and prediction cannot be used with confidence.

Recent NOVA laser and gas gun studies on liquid deuterium by LLNL investigators [2-4] dramatically demonstrate the inadequacy of present models for predicting the pressurization of DT fuels. The LLNL results illustrate that deuterium undergoes a molecular dissociation to a metallic phase at pressures of about 1.4 Mbar and temperatures of about 3000K (present theories predict this transition in the range of 1-20 Mbar at zero Kelvin). A related effect is that under shock compression, dissociation of molecular hydrogen produces a much softer response than predicted by present theories. One consequence is that deuterium is about twice as dense as previously predicted for shock compression to 2 Mbar; this pressure is in the regime that weapons systems and ICF capsules operate. This EOS response was completely unexpected and has profound implications for both the ICF and the weapon physics programs; for ICF, it implies that fusion conditions may be achieved for lower driving pressures in ICF capsules and that the target will be more resistant to Rayleigh-Taylor instabilities.

A major limitation in the NOVA EOS experiments was that the liquid deuterium samples were so small (0.4-mm diameter) that errors in pressure and volume (5-10%) prevent a critical comparison of first-principles theories of molecular dissociation from the experimental results. In contrast, the relatively large sample sizes that are possible for study in Z EOS experiments provide an opportunity to significantly increase the accuracy of EOS measurements and thus allow a critical comparison with theories of molecular dissociation.

### **III. Milestones and Accomplishments for FY97 Phase of Project**

The general plan for the LDRD project “Cryogenic EOS Capabilities on Pulsed-Radiation Sources (Z-Pinch)” [1] was to develop a working cryogenic target system under FY97 LDRD project funding and then to perform EOS measurements on cryogenic samples in FY98 under a continuation of this LDRD or with other funding.

The milestones proposed for the FY97 LDRD phase of the project were the following:

1. Develop a detailed conceptual design for a cryogenic target system that would meet the operational and safety requirements for shock physics experiments on the Z PRS.
2. Evaluate the safety requirements for performing liquid hydrogen experiments on Z.
3. Assemble a cryogenic test facility to perform off-line bench testing of the thermal and optical performance of cryogenic target system components.
4. Design and assemble the appropriate cryogenic hardware and perform initial testing of the cryogenic target system design.
5. Evaluate laser windows for use in cryogenic experiments for wave profile measurements; test the operation of the cryogenics target fixture with VISAR and fiber optics.
6. Integrate the cryogenic target design into the Z facility and test the performance of the system in add-on experiments.

As a result of work covering roughly the period from 2/97-11/97, we have accomplished all of the milestones for the FY97 LDRD phase of this project except for testing of optical EOS diagnostic components at cryogenic temperatures and full integration of the cryogenic target system into the Z facility.

Integration and testing of VISAR optics and fiber optic sensors in the cryogenic target assembly have been delayed because issues concerning operation of these diagnostics at room temperature in the harsh bremsstrahlung environment of Z are still being resolved in a separate research effort [5-7]. As a result, resources required for optical system testing at cryogenic temperatures are presently in use on Z.

We have completed the design of an interface to introduce cryogenic transfer lines, gas lines, and sensor wires into the Z vacuum section and to record sensor output in the Z screenroom. However, integration of the complete cryogenic target system into the Z facility has been delayed because of lack of funds in FY97 for interface components and screenroom instrumentation.

We will elaborate on these accomplishments in each of the following sections.

## **IV. Conceptual Design for Cryogenic Target System**

The basic requirement of any cryogenic cooling system for EOS samples on Z is the ability to cool a compact sample holder which forms part of the secondary hohlraum assembly to a specified temperature  $T$  in the range  $6\text{ K} \leq T \leq 30\text{ K}$ . Sample holders must be designed which are capable of containing liquid samples, including liquid hydrogen ( $\text{LH}_2$ ) and liquid deuterium ( $\text{LD}_2$ ), and solid materials, such as polycarbonate or metallic ablaters for ICF. The liquid sample holder must be capable of containing a liquid at a fixed temperature, with diagnostics to accurately measure the temperature and pressure so that the initial density  $\rho_0$  of the sample can be determined with high precision ( $\pm 0.1\%$ ). The cryogenic target assembly must also include the capability for various shock diagnostics, such as VISAR interferometry, shock velocity measurement, and Raman spectroscopy. For compatibility, the size and access of the cryogenic target assembly must be comparable to the simpler ambient temperature sample holder that has been developed for precision EOS measurements on Z [7]. Possible cooling options include cooling with an  $\text{LH}_2$  reservoir, using a closed-cycle refrigerator, or cooling with a LHe cryostat. A major consideration driving the design is possible damage to the cryogenic system components from radiation and debris as the Z PRS dissipates in excess of 1 MJ of energy in the region of the Z-pinch.

After considering the relevant operational and safety issues, we have concluded [8] that the best approach to cooling an EOS sample on Z is to use a LHe cryostat connected through a cold finger and a thermal link to a sample holder (as shown in Figs. 1 and 2 below) with an automatic temperature control system. The thermal link provides standoff of the cryostat from the sample holder for survivability. The design of the thermal link will depend on the required sample temperature. Wherever possible the high-value cryostat will be enclosed in a blast shield to insure its survival, while the sample holder and associated instrumentation must necessarily be sacrificed on each shot. Using various precision temperature control techniques available for the sample holder, we can access a continuous range of temperatures from about 2 K to 75 K with LHe cooling. Because we are not tied to a narrow temperature range fixed by the boiling point of  $\text{LH}_2$ , for example, this approach is applicable to EOS studies over a broad, continuous range of temperatures.

This approach can be used to generate  $\text{LH}_2$  and  $\text{LD}_2$  samples. The most direct way to form a small ( $1\text{-}2\text{ cm}^3$ )  $\text{LH}_2$  sample is to evacuate and cool a copper sample holder cavity to about 19 K and then condense sufficient  $\text{LH}_2$  from a high purity external hydrogen gas supply to fill the cavity [9,10]. At atmospheric pressure,  $\text{H}_2$  will condense to a liquid in the temperature range between about 15 K and 20.5 K. For  $\text{D}_2$ , this range is about 18 K to 23 K. The sample holder temperature and the pressure of gas over the liquid must be measured. A diagnostic must also be included to provide positive verification that the sample reservoir has been filled with liquid.

In summary, we have developed a detailed conceptual design for a Z-integrated cryogenic target system with the capability for cooling both solid and liquid samples. This system will use LHe cooling and active feedback temperature control to maintain a fixed sample temperature in the range 6 - 30 K. We have designed variations of the cryogenic sample holder to: (1) condense cryogenic liquid samples from the gas phase (specifically  $\text{LH}_2$  and  $\text{LD}_2$  at about 20K); (2) cool solid samples, such as polycarbonate and metallic ablators for ICF studies, to a specified temperature in the range of 6-30 K; and (3) condense solid layers of  $\text{D}_2$  or other materials from the gas phase onto a substrate. Each target assembly includes the capability to use various shock diagnostics, such as VISAR interferometry for particle velocity measurements and optical fibers for shock-breakout measurements of shock velocity. This is a general purpose system in the sense that we can use very similar equipment and techniques to cover a wide range of temperatures and target composition. This system will meet the safety and operational requirements for Z hohlraum experiments. The sample volumes for EOS measurements on Z,

while small, will be much larger than for the NOVA EOS experiments [2], so it should be possible to determine initial and dynamic pressure, temperature, and volume with significantly smaller errors.

## V. Safety Issues

Most of the cryogenic cooling requirements for weapon physics and ICF samples, such as  $\text{LD}_2$ , solid  $\text{D}_2$  and DT, beryllium and CH, could be met by cooling the sample holder with a large  $\text{LH}_2$  reservoir to access the temperature range from  $15 \text{ K} \leq T \leq 23 \text{ K}$ . This technique was used earlier by LLNL for gas-gun EOS measurements [4, 10-12] with few  $\text{cm}^3$  target volumes of  $\text{LH}_2$  and various other condensed gases and involves handling  $\text{LH}_2$  in quantities of several liters indoors at the experiment chamber. Since hydrogen is a flammable, high energy fuel, the safety hazards of handling  $\text{LH}_2$  [13-17] in the Z confined space environment were carefully evaluated in considering this option. Where  $\text{LH}_2$  in a dewar is used for cooling, a leak or spill involving a relatively small (1 - 2 liter) liquid volume can vaporize quickly to form a large volume, flammable  $\text{H}_2$ -air mixture. Such a release in a confined space is always a potentially serious situation, regardless of the level of ventilation. We concluded [8] that the transfer and handling of small (few liter) quantities of  $\text{LH}_2$  in the Z environment represented an unacceptable safety hazard, and that cooling of  $\text{LD}_2$  and other ICF materials should be accomplished with  $\text{LHe}$  cooling and an automatic temperature control system.

A 1 - 2  $\text{cm}^3$   $\text{LH}_2$  sample condensed in a sample holder on Z is not by itself a significant safety hazard. The very small amount of  $\text{LH}_2$  in the sample holder, if released, would be contained inside a blast shield in a large volume vacuum chamber. The main safety hazards in generating small  $\text{LH}_2$  ( $\text{LD}_2$ ) samples then involve the storage, transfer, and venting of the high purity  $\text{H}_2$  or  $\text{D}_2$  feed gas.  $\text{H}_2$  leaks from a gas manifold system normally maintained under high vacuum are quite unlikely and the effects of a small hydrogen gas leak can be easily mitigated by good ventilation.

## VI. Cryogenic Test Facility

We have assembled a cryogenic test facility in the Bldg. 970 Tunnel area to evaluate and refine these cryogenic target system designs. A large volume ( $1.5 \text{ m}^3$ ) vacuum chamber (formerly the SABRE Integrated Test Facility chamber) with 14 large area ports was procured for use as a cryogenic vacuum test chamber. The test chamber vacuum system consists of a roughing pump and a ten-inch cryopump with a gate valve. It is capable of pressures of  $2 \times 10^{-5}$  Torr in about 1 hour and ultimate chamber pressures of about  $2 \times 10^{-6}$  Torr. During cryogenic testing, cryopumping by the cryostat and cryogenic transfer lines have resulted in test chamber pressures as low as  $1.0 \times 10^{-7}$  Torr. Parts for a thermal model of the complete Z-pinch experiment, including the Z anode plate, primary and secondary hohlraums, a plug-in cryogenic sample holder, and a LHe cryostat, have been installed for thermal testing. The LHe transfer and temperature control systems were also assembled. The system is instrumented at present with an array of eight temperature sensors, a LHe level sensor in the LHe reservoir, and pressure gauges to measure the vacuum in the test chamber. Sensor readouts and other instrumentation are housed in an EMI-proof cabinet.

Thermal testing of cryogenic system prototypes with LHe cooling began in 8/97. In initial thermal testing, the unshielded cryogenic sample holder, connected directly to the cryostat through a cold-finger, was cooled to a steady-state temperature of about 5.5 K in 20 minutes. The temperature increase between the cryostat and sample holder was only about 0.5 K, suggesting that a much longer connecting link could be tolerated when cooling the sample holder to 20 K for  $\text{LD}_2$  samples. Under those conditions, the sample holder can be connected to the cryostat through a high conductivity copper cable, with the cryostat protected from destruction behind a debris shield. Based on this thermal testing, we have also been motivated to design an improved cryostat with thermal insulation to allow more efficient use of LHe for temperature control over extended periods.

## VII. Cryostat Design

The cryostat and sample-holder design required for a cryogenic target system in the Z machine environment differs in several important ways from a typical closed laboratory LHe cryostat/sample-holder. The Z cryostat is operated inside a large-volume, high-vacuum ( $2 \times 10^{-5}$  -  $4 \times 10^{-6}$  Torr) environment. This accelerator vacuum is used to provide the initial vacuum

insulation within the cryostat and around the sample holder, so the thermal loading from gas convection will be determined largely by the quality of the Z vacuum. Some improvement in vacuum both inside the cryostat radiation shields and in the Z vacuum section itself can be expected to result from  $\text{LN}_2$  and LHe cryopumping by the cryostat and unshielded cryogenic transfer lines. Cryogenic liquids must be delivered to the cryostat from a location external to the Z vacuum chamber through approximately 4 m of transfer line. Because of the possibility of an extended delay in the shot sequence, the sample holder must be capable of remaining in a stable equilibrium state of temperature and gas pressure for up to 2 hours. Once established, the state of the cryostat and sample holder must be monitored and controlled from a remote screen room through a 70 m cable run. The sample holder, which we wish to cool to a specified temperature in the range of 6-30 K for most applications, must be directly connected to the hohlraum which is initially at room temperature. This hohlraum must be maintained near room temperature during the shot sequence to avoid a change in wire resistivity and to avoid distortion of the wire array geometry by thermal contraction at low temperatures. This requires an effective thermal break between the sample holder and the hohlraum over a distance of about 1 cm. The cryostat together with associated transfer lines and sensor cables, if unprotected, could be destroyed by shrapnel and radiation resulting from the dissipation of more than 1 MJ of energy in the region of the Z-pinch implosion. There is no feasible way to protect the sample holder which is directly connected to the hohlraum, but it is highly desirable to separate the cryostat from the sample holder with a high conductivity thermal link and then enclose the cryostat in an effective debris shield to ensure its survival. Finally, following a shot, the cryostat and associated transfer lines must be warmed rapidly with dry air to allow rapid access and turnaround of the experiment without unnecessary condensation of water vapor on cold components in the Z vacuum section.

For initial thermal testing of cryogenic sample holders, we fabricated two relatively simple and inexpensive continuous flow cryostats. The first cryostat design is shown in Fig. 1. The LHe reservoir is an OFHC copper cylinder. LHe is introduced through a top port and cold He exhaust gas or LHe leaving the reservoir flows through a cooling coil on an inner shield surrounding the reservoir body before exiting the vacuum chamber. The LHe level in the reservoir can be measured with a LHe level sensor inserted through a feedthrough on the top cover. The LHe reservoir and inner shield are each wrapped in a single layer of shiny Al foil to reduce the emissivity and radiational heating of their outer cylindrical surfaces without the expense of polishing and gold plating these surfaces. The



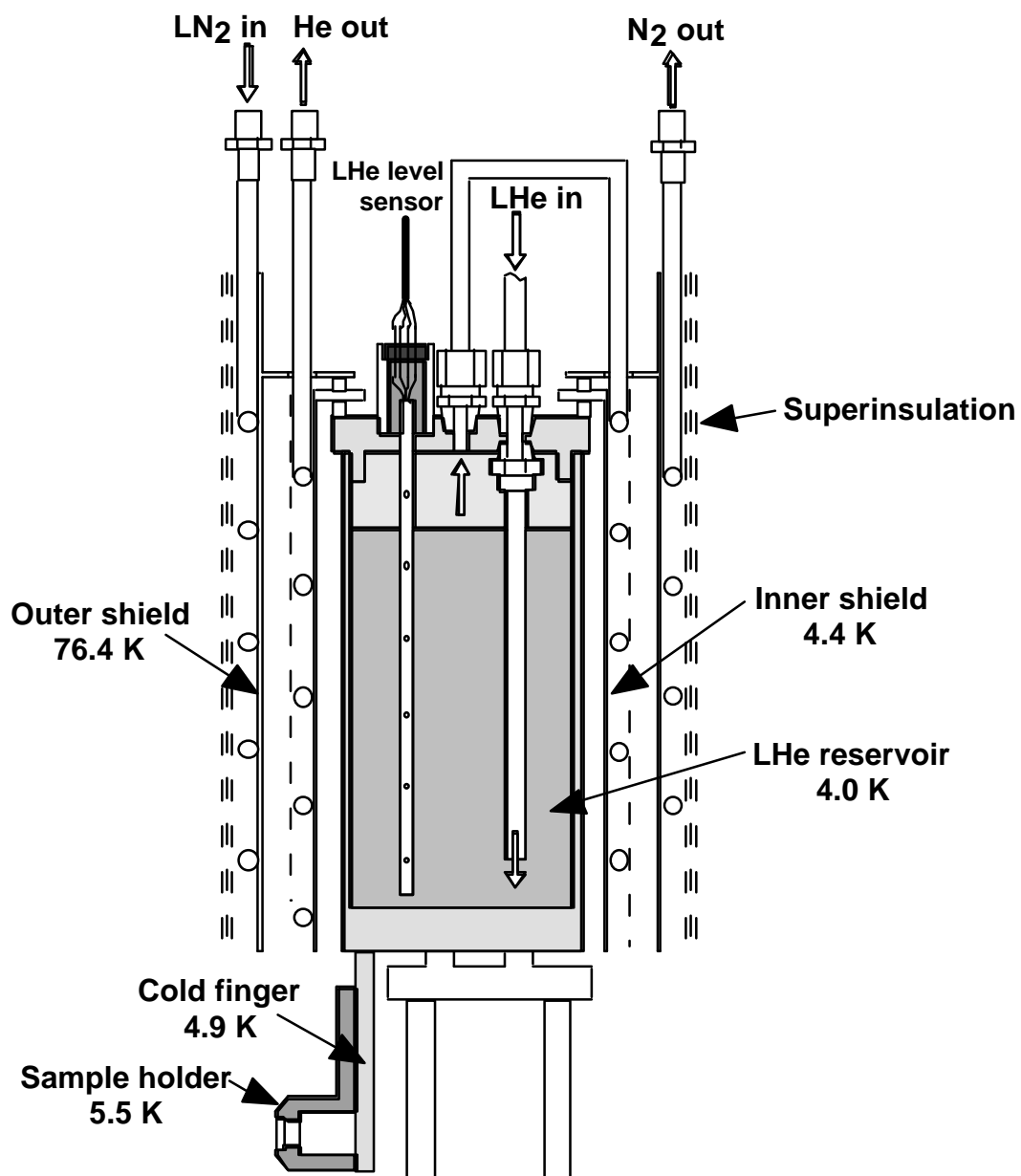


Figure 1. Continuous flow LHe cryostat with LN<sub>2</sub>-cooled outer radiation shield. The sample holder is in direct thermal contact with the cryostat cold finger.

LHe-cooled components are surrounded by an outer,  $\text{LN}_2$ -cooled radiation shield. The outer shield is wrapped in multilayer insulation (25 layers of aluminized-mylar superinsulation) to isolate this shield from the radiation heat load of the surrounding room temperature environment. The sample holder can be bolted directly to the cold finger extending down from the bottom of the LHe reservoir. In this configuration, the unshielded copper sample holder body can be cooled to an equilibrium temperature of 5.5-6.5 K. A second cryostat design shown in Fig. 2 differs from the first cryostat mainly in the placement and shape of the cold finger, which is now a cylindrical extension from the center of the LHe reservoir bottom. In this configuration, the sample holder is connected to the cold finger through a thermal link consisting of a piece of OFHC copper wire. If adequate separation between cryostat and sample holder can be achieved in this way, the high-value cryostat and transfer lines can be enclosed in a debris shield and protected from blast damage.

The main shortcoming of both of these simple cryostats is that they are open at both the top and bottom ends and the LHe transfer lines are not thermally sunked to the shield at  $\text{LN}_2$  temperature. The high heat load on the ends of the LHe reservoir results in relatively rapid evaporation of LHe. As a consequence, the holding time for LHe in these cryostats connected to a sample holder is only about 5 minutes, instead of an hour or more for a fully shielded, more conventional cryostat. However, by continuously flowing LHe through the system, the cryostat can be cooled and maintained at an equilibrium cold-finger temperature of about 5 K for more than an hour using about 50 liters of LHe. This tradeoff of LHe efficiency for ease of cryostat construction proved quite satisfactory in the initial phase of testing where we were interested in quickly defining system requirements. We have recently designed a more conventional and efficient cryostat which is currently being fabricated by a cryogenic equipment manufacturer. This cryostat should have a LHe hold time of an hour or more, depending on the sample heat load, and be more suitable for use on Z. We would like to be able to maintain a steady equilibrium cold finger temperature on Z in a static fill mode (or with continuous LHe flow at a very low flow rate), rather than with a continuous flow system operated at a relatively high flow rate requiring occasional manual adjustment.

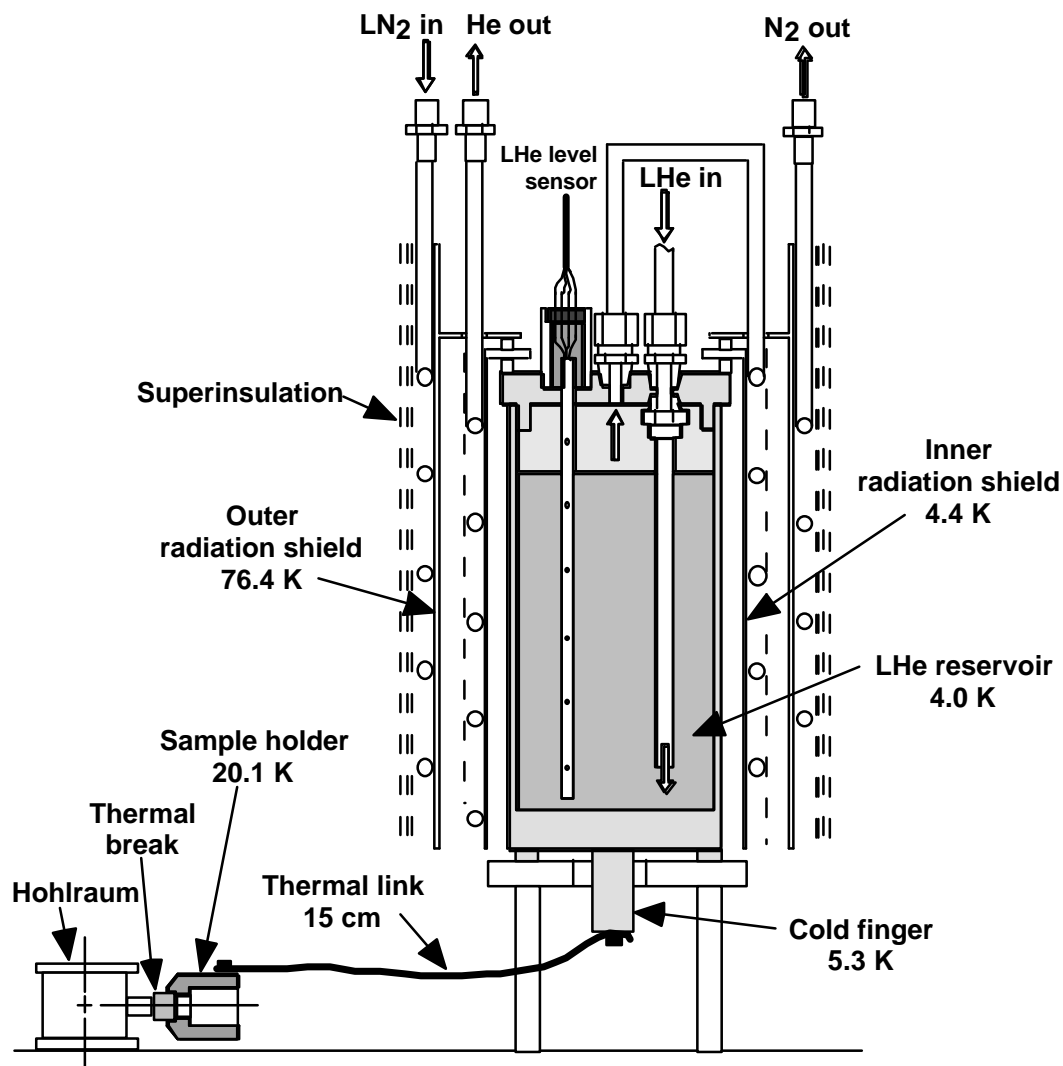


Figure 2. Continuous flow LHe cryostat with LN<sub>2</sub>-cooled outer radiation shield. The sample holder is connected to the cryostat cold finger through a thermal link consisting of OFHC copper wire.

## VIII. Cryogenic Sample Holder Design

Several different cryogenic sample holders have been designed and fabricated to meet the requirements for cooling different types of sample materials. A cryogenic sample holder for containing liquid samples condensed from the gas phase is shown in Fig. 3. The configuration shown could be used for EOS measurements on liquid deuterium ( $\text{LD}_2$ ) condensed from pure deuterium gas within the sample holder maintained at about 20K. The gas is introduced through a fill tube and gas line thermally-sunk to a  $\text{LN}_2$ -cooled surface. Access to shock wave diagnostics is provided through an opening in the back of the sample holder. A thermal break between the sample holder maintained at LHe temperatures and the hohlraum structure which should remain close to ambient room temperature is provided by a nested assembly of copper, stainless steel, and low-conductivity nylon cylinders. The sample holder and thermal break insert directly into the secondary hohlraum, forming a smooth gold-plated radiation channel between the primary

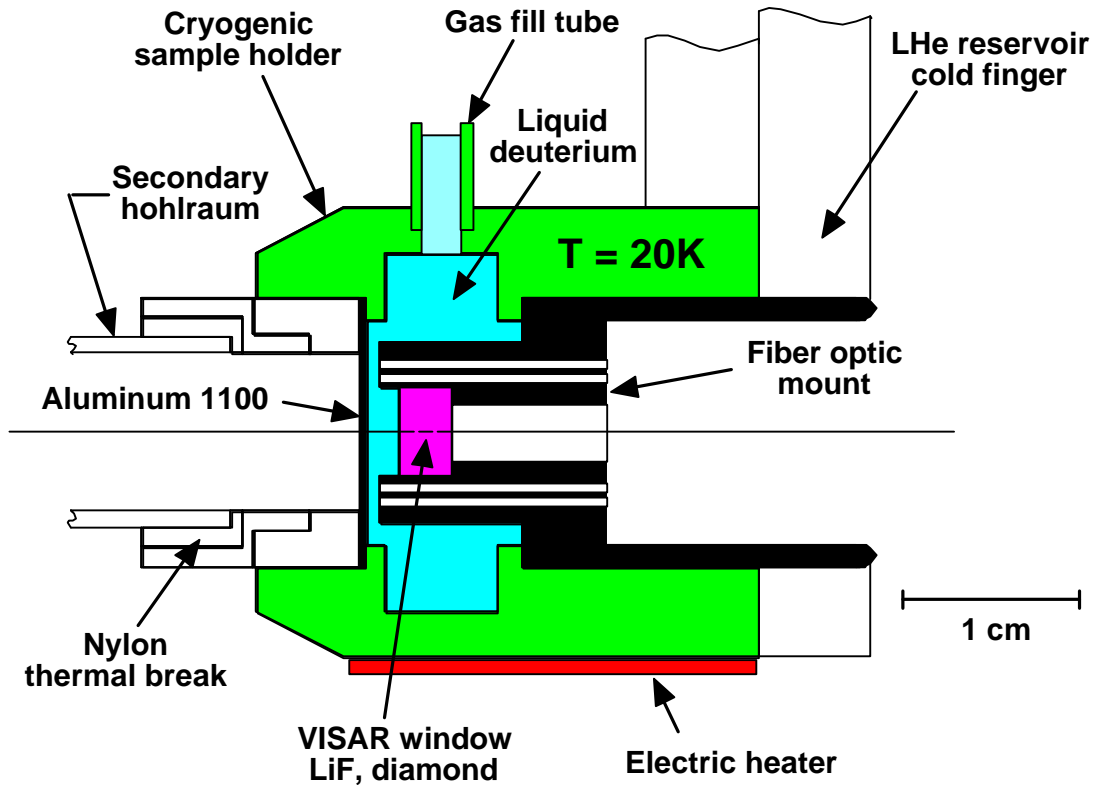


Figure 3. Cryogenic sample holder (OFHC copper) for containing liquid samples ( $\text{LH}_2$ ,  $\text{LD}_2$ ) condensed from the gas phase. A thermal break is provided between the sample holder and hohlraum.

hohlraum and the sample. A second, somewhat simpler cryogenic sample holder for cooling solid samples in the range of about 6-30 K is shown in Fig. 4. Such a sample holder could be used for EOS measurements on Be samples cooled to 18.5 K, for example. If the need should arise for cooling samples in the temperature range of 1.5-5 K, a sample holder with an integrated cryostat, similar to that shown in Fig. 5, could be used. Additional radiation shielding and cooling techniques not shown in the figure would be required to maintain sample temperatures below the normal boiling point of LHe.

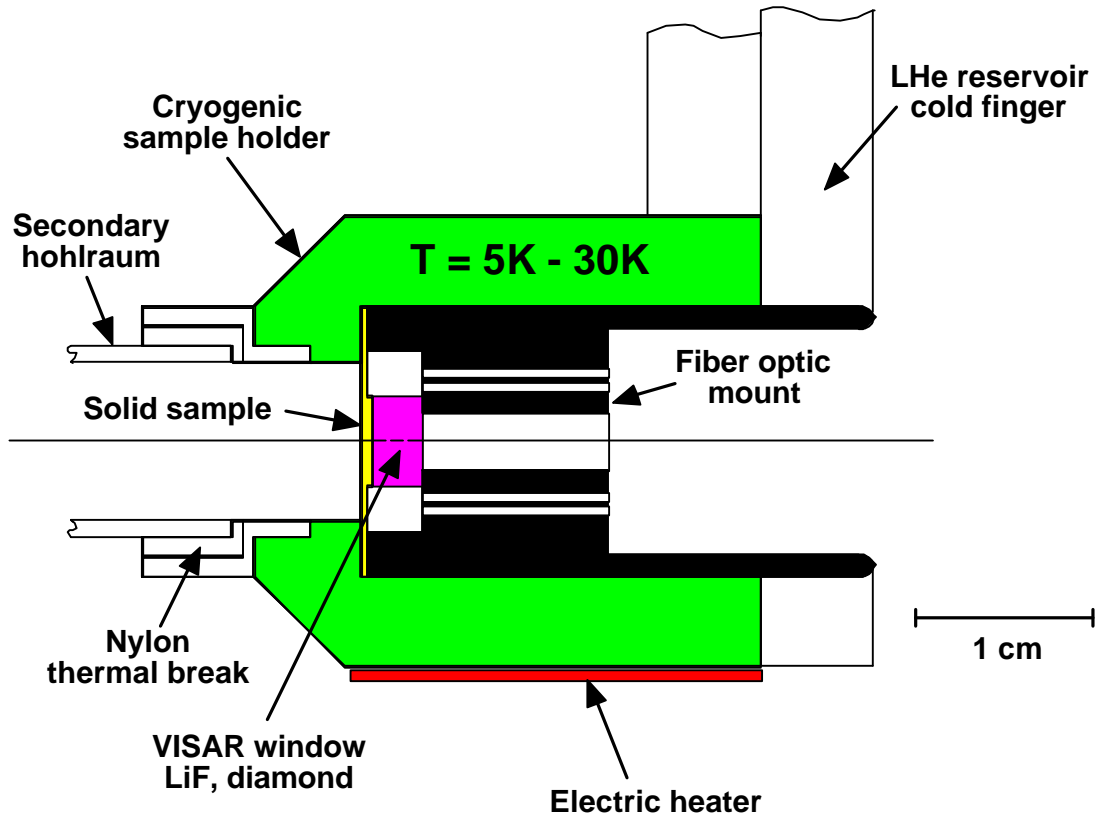


Figure 4. Cryogenic sample holder (OFHC copper) for cooling solid samples in the range of 6-30 K.

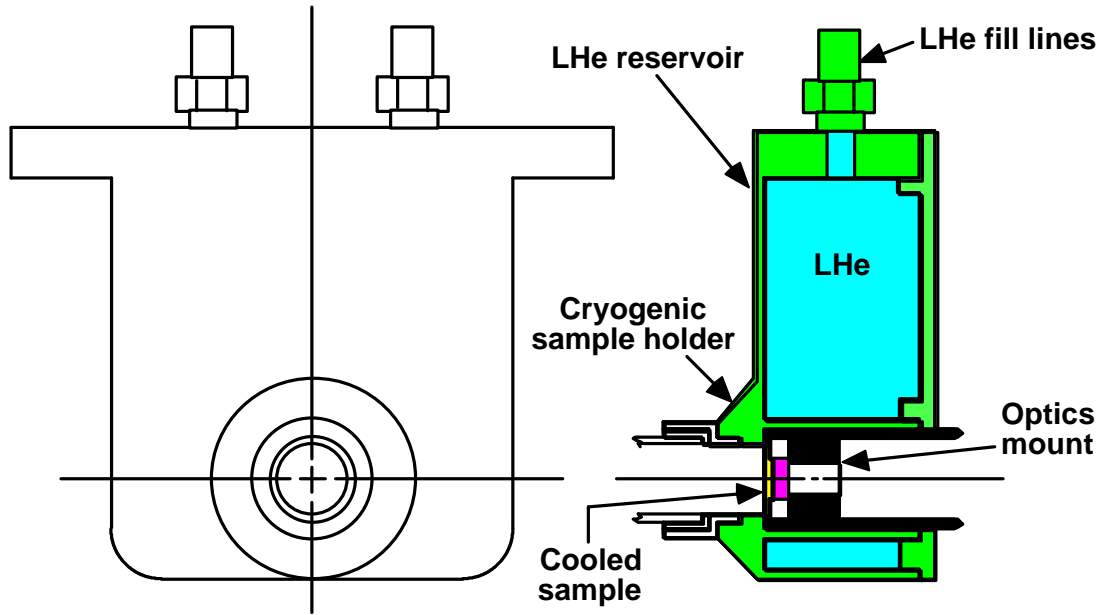


Figure 5. Cryogenic sample holder (OFHC copper) with integrated cryostat for cooling samples to  $T < 6$  K (additional radiation shielding not shown).

## IX. Cryogenic Target System Test Results

Temperature control of the cryogenic sample holder has been demonstrated in a series of cooling tests performed in the cryogenic test facility chamber with the cryostat arrangement shown in Fig. 2 and the sample holder for solid samples shown in Fig. 4. In a typical cooling sequence for the cryogenic target assembly, the cryostat outer shield is first cooled with  $\text{LN}_2$  at full flow rate (40 L/hr) to about 82 K in 8 minutes (Fig. 6). The  $\text{LN}_2$  flow rate is then reduced to less than 10 L/hr.  $\text{LN}_2$  from a 110 L dewar will then flow continuously through the outer shield cooling coil without further attention for many hours. Reducing the  $\text{LN}_2$  flow rate also reduces the pressure in the  $\text{LN}_2$  transfer lines and cooling coil. As a result, the temperature of the outer shield decreases from 82 K to 76.4 K, the approximate boiling point of  $\text{LN}_2$  at atmospheric pressure in Albuquerque. After about 25 minutes, LHe cooling of the LHe reservoir cold finger (Fig. 7) and the inner shield (Fig. 8) is started. These components could be precooled with  $\text{LN}_2$  if efficient LHe use were an important issue. In the present case, these components are cooled entirely with LHe, and reach a temperature below 10 K in about 20 minutes. The cryostat cold finger is connected

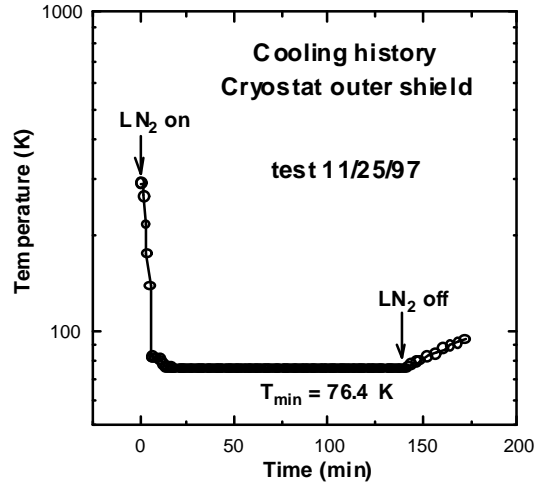


Figure 6. Cooling history of LN<sub>2</sub>-cooled cryostat outer shield (see Fig. 2). Shield temperature decreases from 82 K to 76.4 K as the LN<sub>2</sub> flow rate is reduced from 40 L/hr to 10 L/hr.

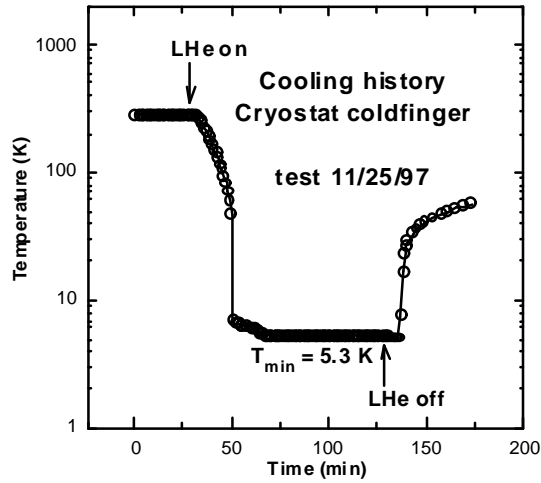


Figure 7. Cooling history of the LHe cryostat cold finger (see Fig. 2) during a temperature control test. The minimum cold finger temperature (5.3 K) is reached after sample holder cooldown to an equilibrium temperature of 20.1 K. The hold-time of the continuous flow LHe reservoir after LHe flow is cut off is about 5 min.

to the sample holder (Fig. 9) through a 15-cm-long, 0.41-cm-diameter section of OFHC copper magnet wire to provide standoff for blast protection of the cryostat. Both the sample holder and the wire thermal link are gold-plated to reduce the radiation heat load at the sample. The sample holder requires approximately 35 minutes after LHe cooling of the cryostat begins to reach its final equilibrium temperature of 20.1 K. The cryostat cold finger and the inner shield do not reach their final equilibrium temperatures of 5.3 K and 4.4 K, respectively, until the sample holder has cooled.

Control of the sample holder temperature stable to within 0.1 K is achieved using a Lakeshore Model 321 Autotuning Temperature Controller. A Kapton-insulated flexible heater (1.3 cm by 5.1 cm, 0.025 cm thick) is silver-epoxied to the body of the sample holder and the sample holder temperature is measured with a silicon diode temperature sensor operated by the temperature controller. A feedback circuit in the temperature controller supplies current to the heater to maintain the sample holder at the temperature setpoint specified by the experimenter. By manually setting the feedback control parameters to appropriate values, small temperature changes of a few K can be accomplished in less than a minute with a minimum of overshoot or seeking by the feedback system. Fig. 10 shows an example of temperature control where the temperature setpoint was increased in a series of 0.5 K steps and then 2.5 K steps to 25.0 K, with the new equilibrium temperature of the sample holder maintained for a few minutes at each setpoint. (This exercise spans the temperature range required to condense LD<sub>2</sub>.) The power required to maintain the sample holder at 25.0 K in this configuration was less than 0.5 W, while the heater can operate at 10 W and the temperature controller is capable of supplying up to 25 W.

The effectiveness of the thermal break (Section VIII) between the sample holder and the hohlraum was evaluated by instrumenting the primary hohlraum top and base mounting flanges with silicon temperature sensors. During the entire cooling sequence for the sample holder, lasting about 3 hours, the primary hohlraum top flange near the secondary hohlraum pipe cooled to only 282.6 K (Fig. 11), a temperature change which will not produce resistivity or dimensional changes in the wire array hardware. The temperature change in the primary hohlraum base flange attached to the heavy anode plate is much smaller. This is a worst case test, as a real Z hohlraum with a mounted wire array would generally contain more thermal mass (larger hohlraum body with wire mounting fixtures) than the model hohlraum for a 17.5 mm wire array employed here.



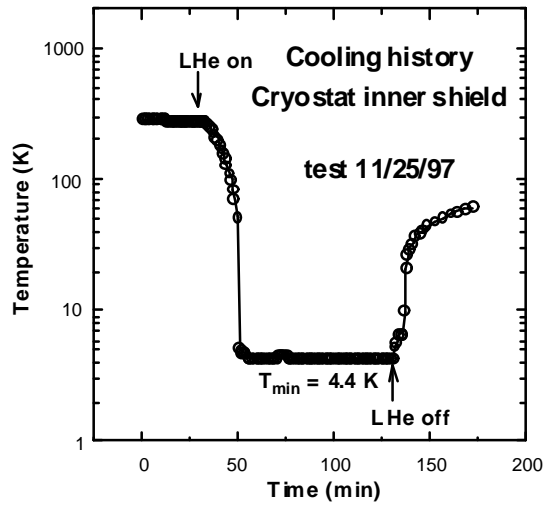


Figure 8. Cooling history of the LHe-cooled cryostat inner shield (see Fig. 2). Minimum temperature (4.4 K) is reached after sample holder cooldown.

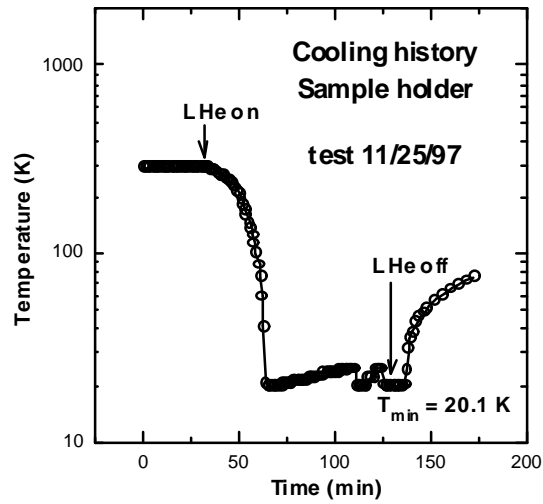


Figure 9. Cooling history of a cryogenic sample holder (Fig. 4) during a temperature control test. The sample holder is connected to the cryostat cold finger through a 15-cm-long, 0.41-cm-diameter section of OFHC copper wire to provide standoff for blast protection of the cryostat (Fig. 2). The sample holder reaches an equilibrium temperature of 20.1 K in this configuration.

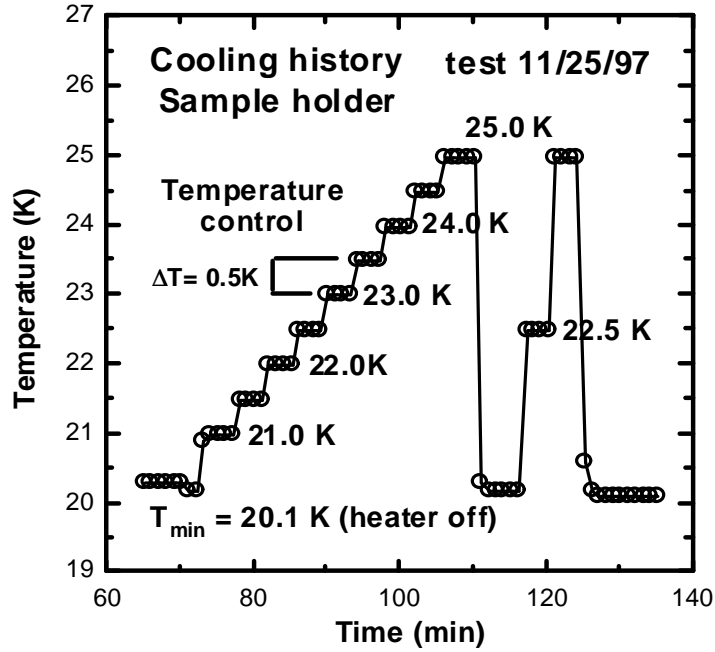


Figure 10. Demonstration of temperature control of the sample holder with standoff (expanded view of Fig. 9). The temperature controller setpoint is increased in 0.5 K steps and then in 2.5 K steps to 25 K and the sample holder temperature is maintained within 0.1 K of the setpoint for several minutes on each step.

Cryopumping by surfaces in the cryostat and by unshielded cryogenic transfer lines should also be expected to improve the vacuum in Z prior to the shot. The magnitude of improvement in the Z vacuum will depend on the duration of cryopumping (delays in the shot sequence will actually help) and on the number and size of machine vacuum leaks present. The improvement in vacuum in the smaller cryogenic test facility vacuum chamber as a result of sequentially cooling the cryostat outer shield with  $\text{LN}_2$  and then the cryostat reservoir and inner shield with LHe is shown in Fig. 12. Starting at a base vacuum pressure of  $1.8 \times 10^{-5}$  Torr (a typical vacuum for Z operation) obtained in about two hours with a single commercial cryopump on the test chamber, a pressure of  $2 \times 10^{-6}$  Torr was

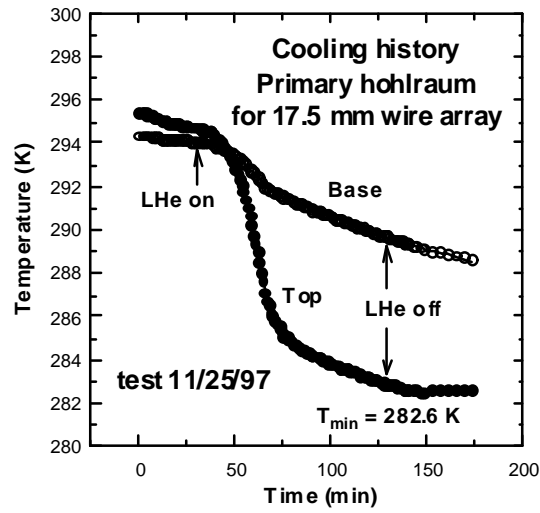


Figure 11. Cooling history of the primary hohlraum connected to the sample holder through the thermal break and secondary hohlraum stub (see Figs. 4 and 9).

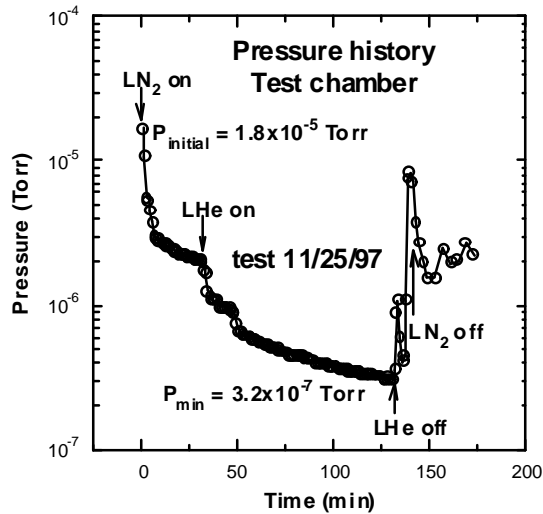


Figure 12. Pressure history in the cryogenic test facility vacuum chamber. The improvement in vacuum is a result of cryopumping by cryogenic target system components during the cooling test (Figs. 6-11).

quickly reached by cryopumping water vapor with  $\text{LN}_2$ -cooled surfaces in the cryostat and a pressure of  $3.2 \times 10^{-7}$  Torr was achieved after about 90 minutes of cryopumping by the LHe-cooled cryostat surfaces. After cryogenic liquid flow is turned off and the cryostat surfaces warm, materials collected on these surfaces are released back into the vacuum, resulting in a large jump in pressure followed by a gradual recovery as the chamber vacuum system pumps away some of the released components.

After the LHe flow is turned off at the end of the test, it requires about 5 minutes for the LHe in the reservoir to boil off before the cold finger temperature (Fig. 7) begins to rise, while the inner shield temperature (Fig. 8) begins to rise immediately as the LHe flow is cut off. We are attempting to develop a well-shielded cryostat where the LHe hold time will be 1 hr or more and the cold finger temperature will not depend on details of the LHe flow through the system.

Some additional insight into the operation of the cryostat and temperature controller can be obtained from data from another cooling test. In this test, a dewar containing about 80 liters of LHe was used to cool the cryostat and sample holder. The cryostat cold finger was connected to the sample holder through a 20-cm-long, 0.41-cm-diameter section of OFHC copper wire. Neither the sample holder nor the wire thermal link were gold plated. In this configuration the sample holder reaches an equilibrium temperature of 24.5 K. Various sample holder temperature control tests were run after cooldown, and then the sample holder was heated very slightly to a setpoint of 25.0 K and maintained at this temperature until the LHe supply ran out. As shown in Fig. 13, the entire LHe cooling sequence from cooldown to exhaustion of the LHe supply (with an elevated heat load from temperature control tests during much of this period) lasted about 3.5 hours. During one temperature control test in this sequence (Fig. 14), the setpoint was increased in 10 K steps to maximum sample holder temperature of 74.5 K to demonstrate that the entire temperature range up to  $\text{LN}_2$  levels could be conveniently accessed with LHe cooling and temperature control. Heater power required to increase the sample holder temperature from an equilibrium value of 24.5 K to 74.5 K was less than 2.5 W.

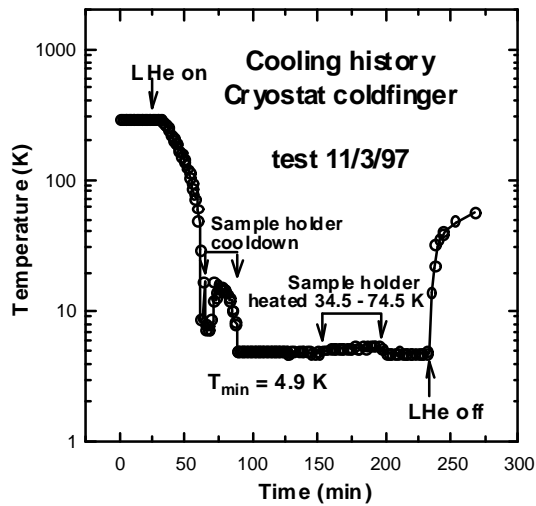


Figure 13. Cooling history of the LHe cryostat cold finger (see Fig. 2) during another temperature control test. The minimum cold finger temperature (4.9 K) is reached after sample holder cooldown to an equilibrium temperature of 24.5 K. LHe consumption during the entire 210 minute LHe cooling sequence from cooldown to exhaustion of the LHe supply was 80 liters.

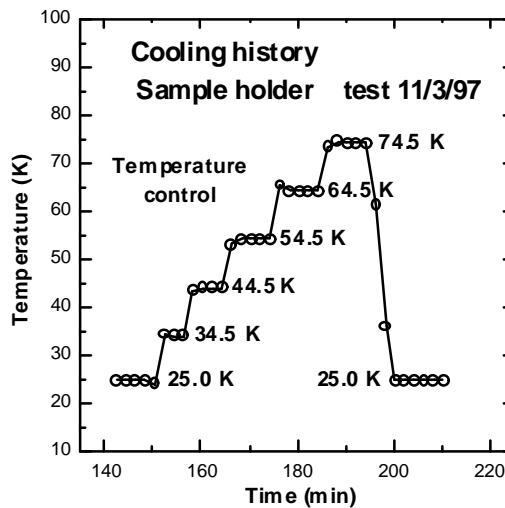


Figure 14. Demonstration of temperature control of the sample holder with standoff. The sample holder is connected to the cryostat cold finger through a 20-cm-long, 0.41-cm-diameter section of OFHC copper wire. The temperature controller setpoint is increased in 10.0 K steps to 74.5 K and the sample holder temperature is maintained within 0.1 K of the setpoint for several minutes on each step.

## **X. Summary and Future Work**

As a result of the FY97 LDRD project “Cryogenic EOS Capabilities on Pulsed Radiation Sources (Z pinch)”, we have made significant progress toward the development of a fully functional general purpose cryogenic target system for precision shock physics measurements on the Z PRS. We have generated a conceptual design and strategy for fielding cryogenic experiments on Z which is shaped by safety considerations and the need for survivability of high-value cryogenic hardware. We have assembled and instrumented a cryogenic test facility, and designed and fabricated cryostats, sample holders, cryogenic transfer, gas delivery, and temperature control systems, and a thermal model of the Z hohlraum. Cooling tests have demonstrated stable cooling of the LHe cryostat cold finger to 5K for greater than 150 minutes, thermal isolation of the sample holder from the hohlraum, spatial standoff of the LHe cryostat from the sample holder for survivability, automatic temperature control of the sample holder, and improvement of the experiment chamber vacuum through cryopumping.

While we have made significant progress in FY97, completion of certain milestones must be extended into FY98 because: (1) initial project funding was delayed until 4/97; (2) issues concerning operation of EOS diagnostics at ambient temperature in the Z bremsstrahlung environment still need to be resolved; and (3) there were insufficient funds in FY 97 to purchase some essential system components.

We must still evaluate the operation of VISAR optics and fiber optics when integrated into a cryogenic sample holder cooled to LHe temperatures. Changes in component dimensions, optical properties, and signal attenuation in cold optical fibers could be important issues for shock physics measurements at low temperatures. Resources needed for optical system testing at cryogenic temperatures were in use at the end of FY97 for dedicated EOS measurements and for diagnostic development add-on shots on Z.

Integration of the cryogenic target system into the Z facility was also delayed because of lack of funds for interface components and screen room instrumentation. An interface to introduce cryogenic transfer lines, gas lines, and sensor wires into the Z vacuum section has been designed and is currently being fabricated. As soon as practical, we must begin integration of the system into the Z facility in preparation for full-scale Z add-on tests of cryogenic system performance.

During initial cryogenic testing, we have been using components which are the approximate thermal equivalent of a real primary hohlraum, secondary hohlraum, EOS target, fiber optic mount, etc. based on current designs. Before cryogenic EOS measurements are attempted on Z in FY98, we must select an optimum primary hohlraum and wire array size based on ongoing Z-pinch source characterization studies, design a secondary hohlraum configuration that can provide uniform temperature across the large EOS sample, and refine the details of the various shock physics target assemblies based on experience gained from EOS measurement on Z with uncooled samples.

## References

- [1] J. R. Asay and D. L. Hanson, "Cryogenic EOS Capabilities on Pulsed Radiation Sources (Z pinch)," 9000 Discretionary LDRD Proposal (FY97), submitted 3/7/97.
- [2] L. B. Da Silva, P. Celliers, G. W. Collins, K. S. Budil, N. C. Holmes, A. Ng, T. W. Barbee Jr., B. A. Hammel, J. D. Killkenny, R. J. Wallace, G. Chiu, and R. Cauble, "Absolute Equation of State Measurements of Shocked Liquid Deuterium up to 200 GPa (2 Mbar)," *Phys. Rev. Lett.* **78**, 483 (1997).
- [3] R. Cauble, "NOVA Experimental Hugoniot of Liquid D<sub>2</sub> up to 2 Mbar," Memo to distribution, LLNL L-22, Livermore CA, 9/9/96.
- [4] N. C. Holmes, M. Ross, and W. J. Nellis, "Temperature measurements and dissociation of shock-compressed liquid-deuterium and hydrogen," *Phys. Rev.* **B52**, 15835 (1995).
- [5] J. R. Asay, "Advanced Shock Wave Diagnostics for Absolute EOS Measurements on PBFA-Z/SATURN at Mbar Pressures," 9000 Discretionary LDRD (FY96) Project Description.
- [6] J. R. Asay, C. H. Konrad, and W. M. Trott, "Ultra-High Pressure EOS Studies on Metals and ICF Ablators using PBFA Z," 9000 Discretionary LDRD Proposal (FY97).
- [7] J. R. Asay, C. H. Konrad, W. M. Trott, C. A. Hall, J. S. Lash, R. J. Dukart, D. L. Hanson, R. E. Olson, G. A. Chandler, L. C. Chhabildas, "Use of Z-Pinch Sources for High Pressure Shock Wave Experiments," *Shock Waves in Condensed Matter 1997 - Proc. of APS 1997 Topical Conf. on Shock Compression in Condensed Matter*.
- [8] D. L. Hanson and R. R. Johnston, "EOS Measurements on PBFA-Z: Conceptual Design for Cryogenic Sample Holder," Memo to J. R. Asay, Sandia National Laboratories, Dept. 9575, 2/4/97.



- [9] K. D. Timmerhaus and M. A. Lechtenberger, "Vapor-Liquid Condensation on Cryogenic Surfaces," *Heat Transfer at Low Temperatures*, W. Frost, ed. (New York: Plenum Press, 1975) pp. 203 - 212.
- [10] W. J. Nellis, A. C. Mitchell, M. van Thiel, G. J. Devine, R. J. Trainor, N. Brown, "Equation-of-state data for molecular hydrogen and deuterium at shock pressures in the range 2 -76 Gpa (20 - 760 kbar)," *J. Chem. Phys.* **79**, 1480 (1983).
- [11] W. J. Nellis and A. C. Mitchell, "Shock compression of liquid argon, nitrogen, and oxygen to 90 Gpa (900 kbar)," *J. Chem. Phys.* **73**, 6137 (1980).
- [12] W. J. Nellis, H. B. Radousky, D. C. Hamilton, A. C. Mitchel, N. C. Holmes, K. B. Christianson, and M. van Thiel, "Equation-of-state, shock-temperature, and electrical-conductivity data of dense fluid nitrogen in the region of the dissociative phase transition," *J. Chem. Phys.* **94**, 2244 (1991).
- [13] *Cryogenics safety manual: a guide to good practice/ Safety Panel, British Cryogenics Council - 3rd Ed.* (Oxford: Butterworth-Heinemann Ltd., 1991) pp.77 - 93.
- [14] *Cryogenic Safety - a summary report of the CRYOGENIC SAFETY CONFERENCE, Allentown, Pennsylvania, July 1959* (Air Products Inc., Allentown, Pa, 1960).
- [15] F. J. Edeskuty, R. Reider, and K. D. Williamson, Jr., "Safety," *Cryogenic Fundamentals*, G. G. Hoselden, ed. (New York: Academic Press Inc., 1971) pp. 633 - 672.
- [16] M. A. K. Lodhi and R. W. Mires, "How Safe is the Storage of Liquid Hydrogen?," *Int. J. Hydrogen Energy* **14**, 35 (1989).
- [17] Kh. S. Kestenboim, G. M. Makhviladze, and A. P. Fedotov, "Evolution of a Cloud of Low-Temperature Light Gas in an Open Atmosphere," *Fluid Dynamics* **26**, 393 (1991).

## Distribution

3	Cornell University	1	MS 1188	C. Wakefield, 9512
	Laboratory of Plasma Studies	1	MS 1182	B. N. Turman, 9512
	Attn: D. A. Hammer	1	MS 1193	J. E. Maenchen, 9531
	B. R. Kusse	1	MS 1193	J. S. Lash, 9531
	J. B. Greenly	1	MS 1193	D. Rovang, 9531
	369 Upson Hall			
	Ithaca, NY 14853			
3	Lawrence Livermore Natl	1	MS 1186	T. A. Mehlhorn, 9533
	Laboratory	1	MS 1186	J. E. Bailey, 9533
	Attn: R. C. Cauble L-041	1	MS 1186	A. L. Carlson, 9533
	G. W. Collins L-481	1	MS 1186	M. Cuneo, 9533
	N. C. Holmes L-050	1	MS 1186	M. P. Desjarlais, 9533
	P. O. Box 808	1	MS 1186	W. Fowler, 9533
	Livermore, CA 94550			
3	Los Alamos National Laboratory	20	MS 1186	D. L. Hanson, 9533
	Attn: R. E. Chrien Jr.	5	MS 1186	R. R. Johnston, 9533
	C. Echdahl	1	MS 1186	P. Lake, 9533
	A. Hauer	1	MS 1186	I. Molina, 9533
	P. O. Box 1663			
	Los Alamos, NM 87545			
3	Naval Research Laboratory	1	MS 1186	T. D. Pointon, 9533
	Attn: G. Cooperstein Code 6700	1	MS 1186	S. A. Slutz, 9533
	P. F. Ottinger Code 6700	1	MS 1186	R. Vesey, 9533
	F. C. Young Code 6770	1	MS 1186	D. F. Wenger, 9533
		1	MS 1182	D. Bloomquist, 9536
1	MS 0151 G. Yonas, 9000	1	MS 1182	B. Lewis, 9536
1	MS 1190 D. L. Cook, 9500	1	MS 1182	D. Petmecky, 9536
1	MS 1195 J. P. Quintenz, 9502	1	MS 1184	J. Boyes, 9539
1	MS 1188 R. Hamil, 9512	1	MS 1184	H. Ives, 9539
1	MS 1188 R. G. Adams, 9512	1	MS 1188	C. L. Olson, 9541
1	MS 1188 D. Bliss, 9512	1	MS 1187	M. K. Matzen, 9571
1	MS 1188 S. Cameron, 9512	1	MS 1187	J. L. Porter, 9571
1	MS 1188 B. F. Clark, 9512	1	MS 1187	M. R. Douglas, 9571

1	MS 1187	T. Haill, 9571	1	MS 1181	C. H. Konrad, 9575
1	MS 1187	B. M. Marder, 9571	1	MS 1196	R. J. Leeper, 9577
1	MS 1187	E. J. McGuire, 9571	1	MS 1196	G. A. Chandler, 9577
1	MS 1187	R. E. Olson, 9571	1	MS 1196	M. S. Derzon, 9577
1	MS 1194	D. H. McDaniel, 9573	1	MS 1196	D. L. Fehl, 9577
1	MS 1194	R. B. Spielman, 9573	1	MS 1196	D. Hebron, 9577
1	MS 1194	K. Baker, 9573	1	MS 1196	T. Nash, 9577
1	MS 1194	C. Deeney, 9573	1	MS 1196	T. Sanford, 9577
1	MS 1194	T. L. Gilliland, 9573	1	MS 1165	J. Polito, 9300
1	MS 1194	J. F. Seamen, 9573	2	MS0188	LDR&D, 4523
1	MS 1194	W. A. Stygar, 9573		Attn: D. L. Chavez	
1	MS 1194	T. Wagoner, 9573	1	MS9018	CTF, 8940-2
1	MS 1194	M. Vargas, 9573	2	MS0899	Tech Library, 4916
20	MS 1181	J. R. Asay, 9575	2	MS0619	R&A Desk, 12690
1	MS 1181	L. Chhabildas, 9575			for DOE/OSTI
1	MS 1181	C. A. Hall, 9575			
1	MS 1181	K. G. Holland, 9575			